Biogeochemistry (2006) 77: 25–56
DOI 10.1007/s10533-005-0712-6

Stabilization of soil organic matter: association with minerals or chemical recalcitrance?

ROBERT MIKUTTA[1,*], MARKUS KLEBER[2], MARGARET S. TORN[2] and REINHOLD JAHN[1]

*[1]Institut für Bodenkunde und Pflanzenernährung, Martin-Luther-Universität Halle-Wittenberg, Weidenplan 14, D-06108 Halle, Germany; [2]Earth Sciences Division, Lawrence Berkeley National Laboratory, Berkeley, California 94720, USA; *Author for correspondence (e-mail: robert.mikutta@landw.uni-halle.de; phone: +49-345-5522456; fax: +49-345-5527116)*

Received 2 February 2005; accepted in revised form 11 July 2005

Key words: C isotopes, Hydrofluoric acid, Lignin, Recalcitrant organic matter, Sodium hypochlorite, Stable organic matter

Abstract. Soil organic matter (OM) can be stabilized against decomposition by association with minerals, by its inherent recalcitrance and by occlusion in aggregates. However, the relative contribution of these factors to OM stabilization is yet unknown. We analyzed pool size and isotopic composition (^{14}C, ^{13}C) of mineral-protected and recalcitrant OM in 12 subsurface horizons from 10 acidic forest soils. The results were related to properties of the mineral phase and to OM composition as revealed by CPMAS ^{13}C-NMR and CuO oxidation. Stable OM was defined as that material which survived treatment of soils with 6 wt% sodium hypochlorite (NaOCl). Mineral-protected OM was extracted by subsequent dissolution of minerals by 10% hydrofluoric acid (HF). Organic matter resistant against NaOCl and insoluble in HF was considered as recalcitrant OM. Hypochlorite removed primarily ^{14}C-modern OM. Of the stable organic carbon (OC), amounting to 2.4–20.6 g kg^{-1} soil, mineral dissolution released on average 73%. Poorly crystalline Fe and Al phases (Fe_o, Al_o) and crystalline Fe oxides (Fe_{d-o}) explained 86% of the variability of mineral-protected OC. Atomic $C_p/(Fe + Al)_p$ ratios of 1.3–6.5 suggest that a portion of stable OM was associated with polymeric Fe and Al species. Recalcitrant OC (0.4–6.5 g kg^{-1} soil) contributed on average 27% to stable OC and the amount was not correlated with any mineralogical property. Recalcitrant OC had lower $\Delta^{14}C$ and $\delta^{13}C$ values than mineral-protected OC and was mainly composed of aliphatic (56%) and O-alkyl (13%) C moieties. Lignin phenols were only present in small amounts in either mineral-protected or recalcitrant OM (mean 4.3 and 0.2 g kg^{-1} OC). The results confirm that stabilization of OM by interaction with poorly crystalline minerals and polymeric metal species is the most important mechanism for preservation of OM in these acid subsoil horizons.

Abbreviations: CPMAS ^{13}C-NMR – cross-polarization magic-angle spinning ^{13}C nuclear magnetic resonance spectroscopy; FR – fluoride reactivity; OC – organic C; OM – organic matter; MOC and MN – mineral-protected organic C and N; ROC and RN – chemically resistant (recalcitrant) organic C and N; SSA – specific surface area; XRD – x-ray diffraction; TEM – transmission electron microscopy

Introduction

Managing soils to increase their carbon storage capacity has been proposed as a means to reduce the rise of CO_2 concentrations in the atmosphere.

Appropriate action, however, requires the understanding of mechanisms governing the long-term residence time of organic matter (OM) in soils. A key element to reliably assessing carbon dynamics is the experimental identification of OM pools linked to the mechanisms of stabilization. Three major factors of OM stabilization have been proposed but the relative contribution of each factor to C protection in soils is unknown (Sollins et al. 1996; Baldock and Skjemstad 2000; Six et al. 2002): (1) physical stabilization relates to the accumulation of OM due to establishing of physical barriers between microbes and enzymes and their substrates as aggregates form (Jastrow et al. 1996; Six et al. 2004); (2) chemical stabilization refers to intermolecular interactions between organic and inorganic substances that decrease the availability of the organic substrate due to complexation of functional groups and changes in conformation (Guggenberger and Kaiser 2003); (3) recalcitrance connotes the preservation of OM caused by structures inherently stable against biochemical decay such as condensed and lignin-derived aromatic carbons, melanoidins, some tannins or aliphatic compounds (Krull et al. 2003; Poirier et al. 2003).

Acid hydrolysis is the procedure most commonly used to isolate stable OM because it preferentially removes young, potentially biodegradable compounds (e.g., proteins, nucleic acids, and polysaccharides) and leaves an old C fraction behind (Leavitt et al. 1996; Paul et al. 1997, 2001). Hence, non-hydrolysable OM has been considered to represent recalcitrant OM (Tan et al. 2004) and its amount has been quoted as a measure for the 'non-active' or 'passive' OM pool (Six et al. 2002; Springob and Kirchmann 2002). This view conveys that stabilization of OM is predominantly the result of its biochemical composition. Acid hydrolysis, however, is inappropriate to distinguish between individual factors of OM stabilization, because non-hydrolysable OM may contain freshly synthesized as well as aged recalcitrant materials (e.g., Balesdent 1996) and, in part, compounds protected by minerals (Leinweber and Schulten 2000).

The importance of minerals for OM stabilization has been demonstrated in incubation experiments, showing slower decomposition rates of OM associated with mineral surfaces (Miltner and Zech 1998; Jones and Edwards 1998; Van Hees et al. 2003; Kalbitz et al. 2005). Also in the field, their importance for long-term OM stabilization has been affirmed by correlations found between the contents of OC and mineral phase properties. For example, in andic soils, poorly crystalline aluminosilicates (allophane, imogolite-type minerals) were shown to account for the sorption and preservation of OM (Torn et al. 1997; Lilienfein et al. 2004). In temperate, non-allophanic soils of varying phyllosilicate composition, Wiseman and Püttmann (2005) observed that C storage was largely a function of the contents of Fe and Al (hydr)oxides.

The objective of the work presented here was to assess quantitatively the contribution of recalcitrant and mineral-protected OM to stable OM in soils of varying mineralogical composition. Our conceptual approach was based on the finding that partial oxidative degradation of OM leaves behind intrinsically resistant as well as mineral-protected organic materials (Theng et al. 1992; Cuypers et al. 2002; Eusterhues et al. 2003; Mikutta et al. 2005). In a previous

study, we estimated stable OM in a set of acid subsoil horizons (i.e., below A horizon) of different mineral composition representing a gradient in mineral surface reactivity (Kleber et al. 2005). The source sites span six soil orders under temperate and tropical forests. Here, we used the same suite of soil samples to study the proportion of mineral-protected and recalcitrant OM in stable OM. Hypochlorite-resistant OM was used as a measure for stable OM because this fraction had a lower ^{14}C content than OM prior to the treatment (Kleber et al. 2005). Following NaOCl treatment, we extracted mineral-protected OM by dissolution of the mineral phase with 10% hydrofluoric acid (HF). We hypothesized that OM left after the NaOCl and HF treatment was largely stabilized by its inherent chemical composition, thus representing recalcitrant (synonymous with chemically resistant) OM. No estimate of OM stabilized by aggregation was possible because of the destruction of soil structure by NaOCl (Omueti 1980) and sieving. We tested our assumptions by investigating (1) the pool sizes and isotopic contents (^{14}C, ^{13}C) of the mineral-protected and chemically resistant OM, (2) the relationship of each OM fraction with mineral phase properties, and (3) the chemical composition of OM using CPMAS ^{13}C-NMR and CuO oxidation.

Materials and methods

Soil materials

Twelve acid subsoil horizons from well-drained sites under neotropical rainforest and temperate mixed deciduous and coniferous forests were selected as described by Kleber et al. (2005) (Table 1). Soil pH (KCl) ranged from 3.3 to 5.8. The sample set spans a wide range of concentrations of crystalline Fe oxides and poorly crystalline Fe and Al phases, includes most of the worldwide abundant phyllosilicate species but excludes allophane and imogolite-type minerals (Table 1). The samples were air-dried, large aggregates were gently broken by hand, and sieved to < 2 mm.

Fractions of stable organic matter

The amount of stable OM was estimated as the amount of residual OM left after treatment with NaOCl (Kleber et al. 2005). Briefly, 10 g of air-dried soil were reacted with 100 ml of 6 wt% NaOCl (Roth, Karlsruhe, Germany), which was adjusted to pH 8.0 by adding 32% HCl. Given the high pH and the prevalence of Na^+ ions, the adsorption of low-molecular-weight compounds produced during NaOCl treatment, like oxalate, to the solids is considered negligible (e.g., Karltun 1998) as is the precipitation of organic compounds with multivalent cations. Three treatment cycles of 6 h each were conducted at 25 ± 1 °C. Samples were centrifuged ($2574 \times g$; 5 min), decanted, and the

Table 1. Properties of subsoil samples.

No.	Classification[a]	Vegetation, age of stands	Horizon	Depth (cm)	Clay (%)	CEC of silicates[b] ($cmol_c\ kg^{-1}$)	SSA[c] ($m^2\ g^{-1}$)	FR[d] (mol $OH^-\ kg^{-1}$)	Fe_t[e] ($g\ kg^{-1}$)	Fe_{d-o}[e] ($g\ kg^{-1}$)	Fe_o[e] ($g\ kg^{-1}$)	Al_o[e] ($g\ kg^{-1}$)	Si_o[e] ($g\ kg^{-1}$)	Phyllosilicate composition[f]
1	Dystric Cambisol	*Fagus sylvatica* L., ~80 years	Bw	5–23	14	6.2	7	0.22	23.0	20.5	2.2	0.8	0.1	I, ML, C, K
2	Haplic Luvisol	*Fagus sylvatica* L., *Quercus petraea*, >150 years	E	5–15	23	15.0	13	0.27	12.6	4.6	1.0	1.2	0.1	V, S, C, HIV, I, K
3	Haplic Luvisol	*Fagus sylvatica* L., *Quercus petraea*, >150 years	Bt	40–80	38	22.5	35	0.47	22.7	8.4	1.0	1.5	0.2	S, HIV, I, ML, K
4	Humic Ferralsol	*Pentaclethra*, lianas, epiphytes, natural Tropical Wet Forest	Bw	75–100	83	4.9	74	0.74	94.8	93.0	1.8	2.8	0.3	H, K
5	Chromic Cambisol	*Picea abies* L. (Karst), *Fagus sylvatica* L., ~105 years	Bw	16–36	62	20.6	32	0.38	50.3	47.3	3.0	2.1	0.1	K, S, C, I
6	Vitric Phaeozem	*Fagus sylvatica* L., 35 years	AB	5–35	27	44.7	40	0.56	63.9	15.3	9.5	3.6	0.9	S, I, C
7	Chromic Cambisol	*Picea abies* L. (Karst), 100 years	Bw	10–30	30	15.5	24	1.30	52.6	17.7	18.7	6.8	0.3	V, HIV, C, K, I

Table 1. Continued.

No.	Classification[a]	Vegetation, age of stands	Horizon	Depth (cm)	Clay (%)	CEC of silicates[b] ($cmol_c\ kg^{-1}$)	SSA[c] ($m^2\ g^{-1}$)	FR[d] (mol $OH^-\ kg^{-1}$)	Fe_t[e] ($g\ kg^{-1}$)	Fe_{d-o}[e] ($g\ kg^{-1}$)	Fe_o[e] ($g\ kg^{-1}$)	Al_o[e] ($g\ kg^{-1}$)	Si_o[e] ($g\ kg^{-1}$)	Phyllosilicate composition[f]
8	Haplic Podzol	*Picea abies* L. (Karst), 50 years	Bhs	10–35	13	6.0	12	0.47	22.7	10.8	9.3	2.2	0.1	I, K, C, V
9	Andic Luvisol	*Picea abies* L. (Karst), ~100 years	Bt	13–33	27	6.7	37	2.01	46.8	22.2	12.5	11.4	1.7	C, ML, I, MH
10	Andic Luvisol	*Picea abies* L. (Karst), ~100 years	2Bw	87–107	18	14.6	30	1.92	49.5	21.9	9.6	10.6	2.5	C, ML, I, MH
11	Umbric Andosol	*Fagus sylvatica* L., *Acer pseudoplatanus* L., *Fraxinus excelsior*, 160 years	Bw	40–70	12	15.5	15	2.86	33.5	5.2	4.9	17.1	4.4	HIV, K, I, C
12	Dystric Cambisol	*Picea abies* L. (Karst), 60 years	Bs	7–22	23	10.8	23	0.71	38.3	20.1	15.7	3.0	0.1	I, K, C, V

[a]According to FAO (1994).

[b]Determined by Na-acetate (pH 7) after treatment with NaOCl and Na-dithionite-citrate.

[c]SSA = specific surface area (BET-N_2) after NaOCl treatment.

[d]FR = fluoride reactivity after NaOCl treatment.

[e]Fe_t = total Fe; Fe_{d-o} = Na-dithionite-citrate-extractable minus NH_4-oxalate-extractable Fe; Fe_o, Al_o and Si_o = NH_4-oxalate-extractable Fe, Al and Si; all extractions after NaOCl treatment.

[f]In order of abundance, abbreviations: I = illite, ML = mixed layer phase, C = chlorite, K = kaolinite, V = vermiculite, S = smectite, HIV = hydroxy-interlayered vermiculite, MH = metahalloysite, H = halloysite.

residues washed twice using 100 ml 1 M NaCl and shaken overnight with deionized water before dialysis (Medicell International; 12–14,000 Da). When the electrical conductivity was < 40 μs cm^{-1}, the samples were freeze-dried.

The NaOCl-treated samples were subsequently extracted with HF in order to dissolve mineral constituents and attached OM. Three grams of freeze-dried sample were transferred into pre-weighed centrifuge bottles and treated four times with 20 ml 10% HF. The samples were shaken for 2 h, centrifuged ($2574 \times g$; 10 min), and the supernatant discarded. The residues were washed five times with 20 ml deionized water, freeze-dried, and the weights recorded. The non-extractable organic carbon and nitrogen were defined as chemically resistant (= recalcitrant) (ROC/RN). After HF treatment, the absolute amount of ROC/RN was calculated utilizing the OC/N content measured in the sample residuum, and the weights of the initial and residual sample; contents were expressed on a bulk soil basis (g kg^{-1} soil). The amount of HF-extractable OC/N (mineral-protected OC/N; MOC/MN) was calculated by subtracting the OC/N contents of the ROC/RN fraction from those of the stable fraction.

Isotopic analysis

Radiocarbon contents of untreated OM and of OM obtained after NaOCl or NaOCl plus HF treatment were measured on graphite targets by accelerator mass spectrometry. Targets were prepared by zinc reduction as described by Kleber et al. (2005). The $\Delta^{14}C$ values and conventional ^{14}C age values were calculated according to Stuiver and Polach (1977). Following archeological protocol, conventional radiocarbon ages were calculated using the Libby half-life (5568 years; mean life 8033 years) rather than the correct value of 5730 years (Stuiver and Polach 1977) and were referenced to 1950 such that 1950 A.D. = 0 B.P. Samples with more ^{14}C than the 1950 atmosphere (after ^{13}C-corrections) are labeled modern. For these reasons, but primarily because soil OM is a continuously cycling pool, the radiocarbon age of OM does not represent how long the material has been in the plant-soil system, and a difference in ages does not give an absolute difference in residence time. It does, however, provide a unique, quantitative measure of the radiocarbon content that can be used to compare quantitatively among pre-modern samples. Also, conventional radiocarbon age does provide a qualitative indication of C residence time and stability. The isotopic content (I) of extracted OC pools could not be measured directly. Thus, $\Delta^{14}C$ values and the 'fraction modern' (F) of NaOCl-removable OC (LOC; labile towards NaOCl) and HF-removable OC (MOC) were calculated from mixing models (Equations 1 and 2),

$$\text{I-C}_\text{L} = [(\text{I-C}_\text{U} \times \text{UOC}) - (\text{I-C}_\text{S} \times \text{SOC})]/\text{LOC} \quad (1)$$

$$\text{I-C}_\text{M} = [(\text{I-C}_\text{S} \times \text{SOC}) - (\text{I-C}_\text{R} \times \text{ROC})]/\text{MOC} \quad (2)$$

where $I\text{-}C_U$, $I\text{-}C_L$, $I\text{-}C_S$, $I\text{-}C_M$ and $I\text{-}C_R$ are either F or $\Delta^{14}C$ values of untreated, NaOCl-removable, NaOCl-resistant (stable), mineral-protected and chemically resistant OM; respectively, and UOC, LOC, SOC, MOC and ROC correspond to the respective OC contents. The ^{14}C ages of LOC and MOC were estimated by using Equation 3, where τ is the Libby mean life (8033 years).

$$^{14}C \text{ age (years)} = -\tau \ln F \quad (3)$$

Before graphitization, CO_2 splits were taken to determine the $\delta^{13}C$ of untreated, total stable, and chemically resistant OM. The $\delta^{13}C$ values were expressed in per mil relative to the Pee Dee Belemnite standard (PDB). Precision of measured $\delta^{13}C$ values was better than 0.1‰. The $\delta^{13}C$ values of the LOC and MOC fraction were calculated by mixing models as described above.

Lignin analysis

Untreated samples and samples treated either with NaOCl or NaOCl plus HF were analyzed in duplicates for lignin phenols by CuO oxidation as described in Amelung et al. (1999). Lignin phenols were measured by capillary gas chromatography (GC-2010, Shimadzu Corp., Tokyo, Japan) equipped with a fused silica SPB-5 column (30 m, 0.25 mm inner diameter, 0.25 μm film, Supelco). The temperature program was set as follows: heating to 100 °C for 3 min, heating to 250 °C (rate: 10 °C min^{-1}), 10 min at 250 °C, heating to 300 °C (rate: 30 °C min^{-1}), and 8 min at 300 °C. Lignin phenols were identified and quantified according to the retention times and response factors of external phenol standards. As internal recovery standards, ethyl vanillin was added prior to CuO oxidation and phenylacetic acid prior to derivatization. The concentrations of phenols were corrected for losses of ethyl vanillin (average recovery: 82%). Vanillyl (V) and syringyl (S) units were calculated from the concentrations of their respective aldehydes, carboxylic acids, and ketones: $V = \sum$ (vanillin + vanillic acid + acetovanillone), $S = \sum$ (syringaldehyde + syringic acid + acetosyringone). Cinnamyl units (C) were derived from the summed concentration of ferulic acid and *p*-coumaric acid. Total content of lignin-derived phenols (VSC) was determined by the sum of structural units: $VSC = \sum (V + S + C)$.

Solid-state cross-polarization magic angle spinning carbon-13 NMR

The ^{13}C-NMR spectra of chemically resistant OM was recorded using a Bruker DSX 200 spectrometer (Bruker BioSpin GmbH, Rheinstetten, Germany) at a ^{13}C resonance frequency of 50.3 MHz, using the cross-polarization magic-angle spinning (CPMAS) technique as described in Gonçalves et al. (2003). The ^{13}C chemical shifts were referenced to tetramethylsilane (= 0 ppm). For

estimation of the distribution of functional groups, eight chemical-shift regions were integrated separately (Knicker and Lüdemann 1995; Table 6).

Other analysis

The total OC and N content of freeze-dried samples was measured by dry combustion at 1150 °C using a Vario EL CNS analyzer (Elementar Analysensysteme, Hanau, Germany). For determination of the H/C ratios of OM left after NaOCl plus HF treatment, H and C of freeze-dried samples were analyzed by dry combustion at 900 °C with a Leco-932 CHNS analyzer (Leco Corp., St Joseph, USA). The fluoride reactivity (FR) of samples after NaOCl treatment, representing the amount of OH^- ions released from mineral surfaces by reaction with NaF, was determined as described in Kleber et al. (2005). The cation exchange capacity of silicates was estimated after treatment with NaOCl and Na-dithionite-citrate by saturating the soil with 1 M Na-acetate (pH 7) and extracting the retained Na with 1 M NH_4-acetate at pH 7. The extracted Na was measured by flame-emission photometry at 570 nm (ELEX 6361, Eppendorf, Hamburg, Germany). The CEC was corrected for residual OM: CEC of silicates ($cmol_c\ kg^{-1}$) = CEC ($cmol_c\ kg^{-1}$) – [2 × OC ($g\ kg^{-1}$) × 500 ($cmol_c\ kg^{-1}$)/1000], where CEC is the determined CEC, 2 is a conversion factor to transform OC into OM contents, and 500 $cmol_c\ kg^{-1}$ is the CEC assumed for residual OM.

Total content of Fe (Fe_t) was determined by X-ray fluorescence (SRS 3000, Siemens AG, Karlsruhe, Germany). After NaOCl treatment, dithionite-citrate-extractable Fe (Fe_d) and oxalate-extractable Fe (Fe_o), Al (Al_o) and Si (Si_o) were determined according to Blakemore et al. (1987). Element concentrations in extraction solutions were measured by inductively coupled plasma atomic-emission spectroscopy (ICP-AES; Yves Yobin JY 70 plus). Pyrophosphate-extractable Fe (Fe_p) and Al (Al_p) were determined at a soil:solution ratio of 1:100 (wt: v) in 0.1 M $Na_4P_2O_7 \cdot 10H_2O$. The mixtures were shaken for 16 h and 5 ml of 50 mM $MgSO_4$ were added to induce flocculation. The suspensions were centrifuged (8183 × *g*; 15 min), the supernatants filtered through 0.45-μm PVDF (polyvinylidene fluoride) syringe filters, and Fe and Al were measured by ICP-AES. The amount of pyrophosphate-extractable OC (C_p) was determined by persulfate-UV oxidation (Foss-Heraeus LiquiTOC). All element contents were normalized to 105 °C dry soil. Dithionite-citrate extractable Fe represents both crystalline and poorly crystalline Fe oxides. Oxalate-extractable Fe, Al, and Si represent poorly crystalline aluminosilicates, ferrihydrite, and Al and Fe in organic complexes, whereas Fe_{d-o} is a measure for the content of crystalline Fe oxides. Pyrophosphate-extractable Fe and Al are usually taken to represent the amount of Fe and Al complexed with OM (Oades 1989).

After NaOCl plus HF treatment, X-ray diffraction on powder specimens was performed for identification of minerals using a D5005 instrument (Siemens AG, Karlsruhe, Germany) with CuKα radiation (40 kV; 30 mA) of wavelength

0.15406 nm, a step size of 0.5° (2Θ), and a step time of 10 s. Surface area analysis was done on the soil mineral fraction by N_2 adsorption at 77 K using a Nova 4200 analyzer (Quantachrome Corp., Boynton Beach, USA). Hypochlorite-treated < 50 μm-fractions were preconditioned by 16 h freeze-drying and 2 h degassing at 10^{-3} mbar. The specific surface area (SSA) was determined by the BET approach applied to five adsorption points in the relative pressure range of P/P_0 0.05–0.30 (Brunauer et al. 1938). The reported SSA data were corrected for the weight of residual OM: SSA_{CORR} ($m^2\ g^{-1}$) = SSA_{BET} ($m^2\ g^{-1}$) × (1 − [2×OC (g kg^{-1})/1000]), where SSA_{BET} refers to the measured SSA and 2 is a conversion factor to transform OC into OM contents. Separated samples were examined by scanning electron microscopy (JOEL JSM 6300) and transmission electron microscopy (JOEL JEM 1210), both in combination with energy dispersive X-ray diffraction (EDX). For TEM investigations, we used sonicated fine clay fractions (< 0.2 μm) dried on SiO_2-coated Cu-nets (200 mesh).

Statistics

Statistical analyses were performed using STATISTICA for Windows 5.1. Ordinary least-square single and multiple linear regression were used to examine the relationships of OM fractions with mineral phase variables. Before performing regressions, the normality of variables representing the properties of the mineral phase and of OM were tested by the Kolmogorov–Smirnoff Test. The significance of differences between treatment means was tested by a paired Student's *t*-test.

Results

Mineral-protected organic matter

In the subsoil samples, the amount of OC left after NaOCl treatment, ranging from 2.4–20.6 g kg^{-1} soil, comprised on average 49 ± 16% of the initial OC. Hypochlorite-resistant N accounted for 0.3–0.9 g kg^{-1} soil and represented 55 ± 26% of the initial N (Kleber et al. 2005; Table 2). Mineral dissolution by 10% HF reduced the sample dry matter by 74–99 wt% (mean value 92 ± 7 wt%) and quartz and newly synthesized ralstonite ($NaAlMgF_6 \cdot H_2O$) were the prevailing minerals. Except for some muscovite, no 0.7–1.8 nm phyllosilicates survived the HF treatment.

Hydrofluoric acid treatment released 40–96% of the stable OC (mean value 73 ± 15%) and 69–97% of stable total N (mean value 87 ± 7%) (Table 2; Figure 1a). There were significant correlations between HF-soluble stable OC (MOC) and oxalate-extractable Fe_o ($r^2 = 0.56$; $p < 0.01$), Al_o ($r^2 = 0.45$; $p < 0.05$), and $(Fe + Al)_o$ ($r^2 = 0.78$; $p < 0.001$; Figure 1b). Mineral surface

Table 2. Total organic C (OC), nitrogen (N), and C/N ratios of OM fractions.

No.	Untreated			NaOCl-resistant										
				Total			Released by HF (MOC)				Not released by HF (ROC)			
	OC ($g\ kg^{-1}$)	N ($g\ kg^{-1}$)	C/N[a]	OC ($g\ kg^{-1}$)	N ($g\ kg^{-1}$)	C/N[a]	OC ($g\ kg^{-1}$)	N ($g\ kg^{-1}$)	C/N[a]	% of total	OC ($g\ kg^{-1}$)	N ($g\ kg^{-1}$)	C/N[a]	H/C[b]
1	10.8	0.7	15	4.8	0.5	10	3.4	0.5	7	71	1.4	0.03	46	2.4
2	11.5	0.7	16	4.2	0.3	15	2.5	0.3	9	61	1.7	0.03	59	2.1
3	4.9	0.3	16	2.4	0.3	8	1.4	0.3	6	59	1.0	0.05	22	4.7
4	10.0	0.9	11	8.7	0.9	9	7.6	0.8	10	87	1.1	0.11	11	N.A.
5	19.7	1.6	12	6.1	0.7	9	4.0	0.6	7	66	2.1	0.1	20	3.6
6	38.2	2.3	17	10.7	0.6	19	4.2	0.4	10	40	6.5	0.19	35	6.6
7	36.0	1.9	19	20.6	0.8	24	16.4	0.7	23	80	4.2	0.09	46	2.5
8	13.8	1.0	14	6.3	0.8	7	4.7	0.7	7	74	1.6	0.1	17	3.5
9	30.7	1.6	19	17.7	0.5	34	12.4	0.4	30	70	5.3	0.08	63	2.2
10	15.7	1.4	11	9.0	0.6	15	7.9	0.5	15	88	1.1	0.06	17	5.9
11	27.7	2.0	14	14.2	0.7	19	11.4	0.6	19	80	2.8	0.1	28	6.4
12	23.2	1.3	18	10.0	0.6	16	9.6	0.6	17	96	0.4	0.02	20	2.2

The stable OC resisting treatment with NaOCl and subsequently released by HF refers to mineral-protected OM, whereas OC not released by HF represents chemically resistant (recalcitrant) OM.

[a]Weight ratios.

[b]Atomic ratios.

N.A.: not available because insufficient amount of sample for analysis.

hydroxyls, as primarily released from aluminol (≡Al–OH) groups by reaction with NaF, were also related to MOC ($r^2 = 0.49$; $p < 0.05$). The SSA and CEC of silicates did not correlate with MOC ($r^2 = 0.01$ and 0.07, respectively), denoting that there is no direct proportionality between the size of mineral surfaces or the charge of siloxane surfaces with the amount of mineral-protected C. However, the SSA values of samples 2, 3 and 6, which all contain smectite with large internal surfaces in pores < 2 nm (Table 1), may have been underestimated. Nitrogen diffusion into interlayer regions of the smectite was probably restricted since the interlayers may have collapsed following treatment with Na^+ (Rutherford et al. 1997) and drying. Whereas we observed a poor relation between MOC and crystalline Fe oxides (Fe_{d-o}) in a single linear regression model ($r^2 = 0.001$), the combination of Fe_o, Al_o, and Fe_{d-o} explained 86% of the MOC concentration variability within a multiple linear regression model (Equation 4; partial correlation coefficients and p values for Fe_o, Al_o and Fe_{d-o} are: $r = 0.85$, $p < 0.01$; $r = 0.80$, $p < 0.01$; and $r = 0.60$, $p < 0.07$, respectively).

$$\text{MOC } (\text{g kg}^{-1}) = 0.50\ \text{Fe}_o + 0.47\ \text{Al}_o + 0.05\ \text{Fe}_{d-o} - 0.34 \quad (R^2 = 0.86; p < 0.001; n = 12) \tag{4}$$

Thus, crystalline Fe oxides contribute to the overall variability of MOC concentration, while they fail to predict the MOC content as a single independent variable. The most likely reason for that is illustrated in Equation (5) and Figure 2, showing that in samples relatively high in crystalline Fe oxides and low in oxalate-extractable Fe and Al compounds [Samples 1–5 with $Fe_o/Fe_d < 0.2$ and $(Fe + Al)_o < 10$ g kg^{-1}], MOC might be primarily associated with crystalline Fe oxides. This is most obvious for the Humic Ferralsol Bw horizon, which contained well-crystalline goethite and hematite and only a marginal concentration of active Fe ($Fe_o/Fe_d < 0.02$).

$$\text{MOC } (\text{g kg}^{-1}) = 0.06\ \text{Fe}_{d-o} + 1.66 \quad (r^2 = 0.93; p < 0.01; n = 5) \tag{5}$$

Crystalline minerals exhibit smaller SSA values and hydroxyl site densities than poorly crystalline minerals (Bracewell et al. 1970), and thus are less efficient in forming organo-mineral associations than poorly crystalline minerals. Consequently, crystalline Fe oxides need to be present in substantial amounts (> 45 g kg^{-1} soil; Figure 2) to protect similar proportions of OM as samples containing moderate amounts of poorly crystalline minerals (e.g., Samples 6 and 8).

Transmission electron microscopy of the fine-clay fraction (< 0.2 μm) of the Chromic Cambisol Bw horizon (Sample 7; highest Fe_o content of all studied samples; Table 1) revealed that stable OC was primarily bound to microcrystalline Fe oxides, likely corresponding to ferrihydrite (Figure 3a). The abundance of ferrihydrite in all horizons is indicated by Fe_p/Fe_o ratios ranging from 0.1–0.6 (mean at 0.4). Compared with sample 7, in the Umbric Andosol Bw

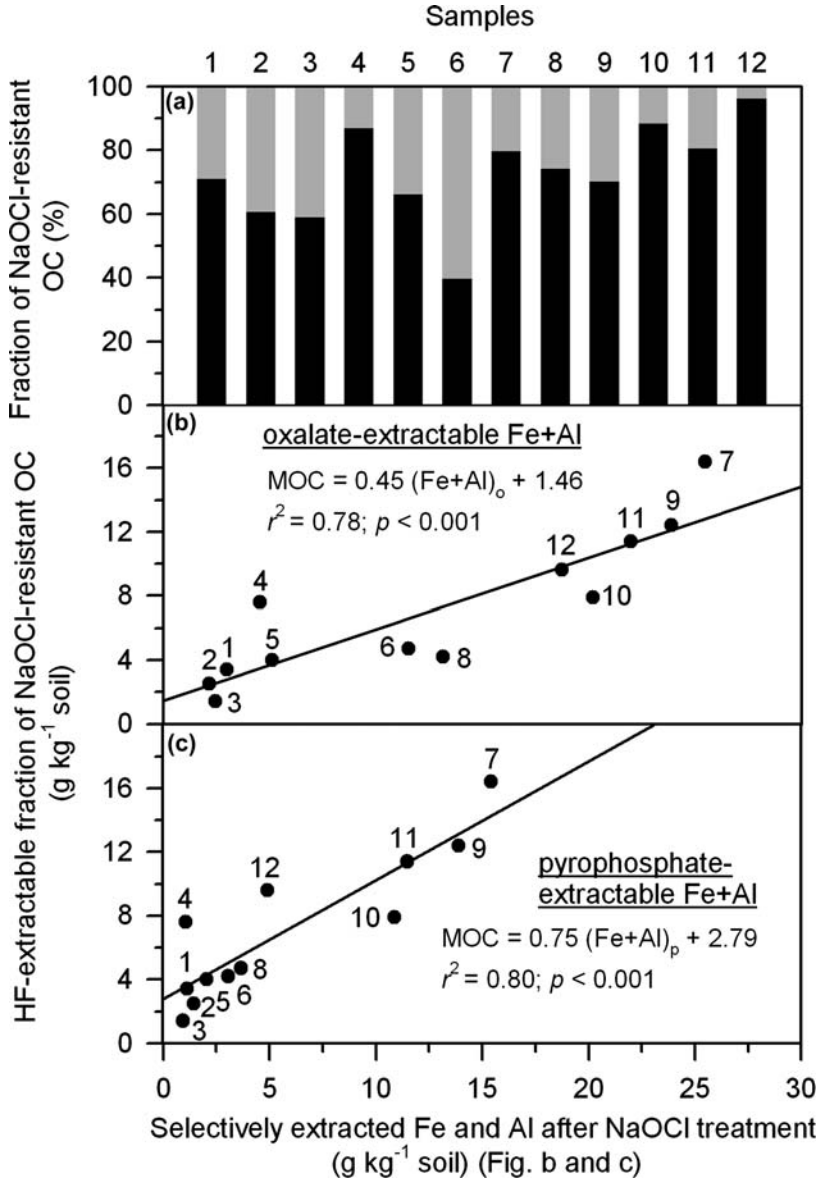

Figure 1. (a) Relative contribution of mineral-protected (black bars) and chemically resistant (recalcitrant) OC (gray bars) to stable OC in acid subsurface horizons. Stable OC is the fraction of OM surviving treatment with NaOCl. Mineral-protected OC was subsequently released by treatment with HF, whereas chemically resistant OC was not extracted by HF. (b) and (c) Relation of selectively extracted Fe plus Al contents with the concentration of mineral-protected OC (MOC). Average analytical errors, expressed as coefficients of variation, of $(Fe + Al)_o$, $(Fe + Al)_p$, mineral-protected and chemically resistant OC among all twelve samples analyzed were 8, 2, 2, and 2%, respectively. Sample labeling corresponds to Table 1.

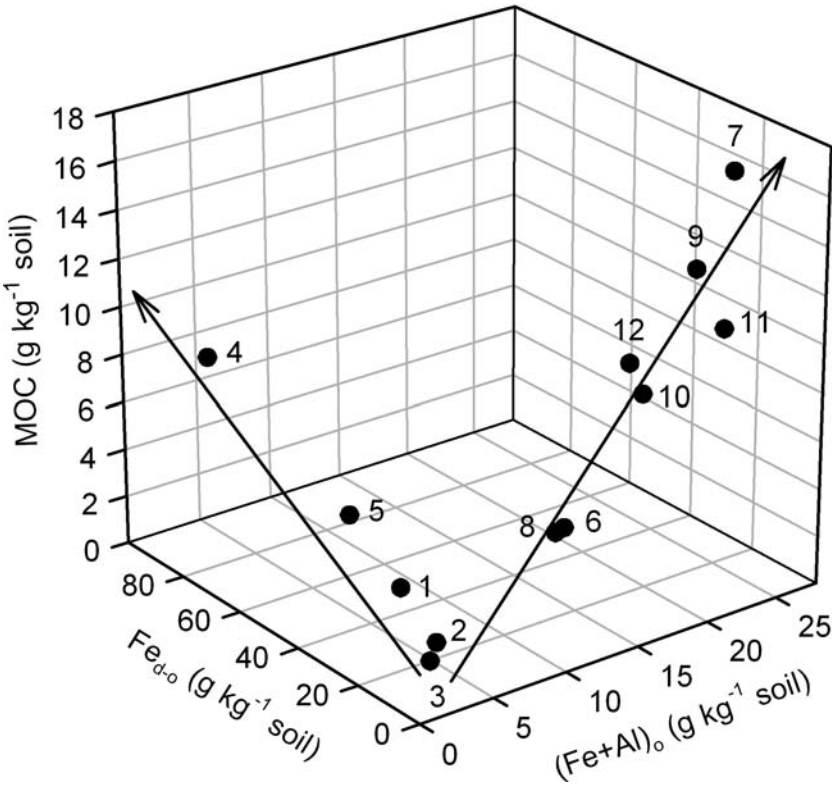

Figure 2. Three-dimensional plot showing the relation of the content of mineral-protected OC (MOC) with the contents of Fe and Al extracted from poorly crystalline minerals and metal-humus complexes [$(Fe + Al)_o$] and crystalline Fe oxides (Fe_{d-o}). In samples 1–5, where little poorly crystalline minerals are present ($Fe_o/Fe_d < 0.2$), a significant relationship of MOC with Fe_{d-o} ($r^2 = 0.93$) suggests that MOC is mainly associated with crystalline Fe oxides. Arrows are displayed for better visualization only. Sample labeling corresponds to Table 1.

horizon (Sample 11; highest Al_o content; Table 1), TEM-EDX showed that a larger fraction of stable OC was related to Al-containing mineral phases (Figure 3b). Despite this, amorphous or poorly ordered Al hydroxides, as suggested by the high Al_o content, could hardly be identified by TEM. Given an average Al_p/Al_o ratio of 0.6 in the studied horizons (range 0.3–0.8), a larger fraction of Al probably resides in organic complexes. In both samples examined by TEM, crystallites of Fe oxides, often as small as 2–10 nm in diameter, were observed as either coverages on silicate platelets (Figure 3c and d), agglomerations (Figure 3e) or, as shown by EDX analysis, inside of C-, Al-, and Si-enriched microaggregates (Figure 3f).

Theoretically, extraction with Na-pyrophosphate following NaOCl treatment should release stable OM protected against oxidative degradation by complexation with Fe and Al species. Pyrophosphate extracted 22–61%

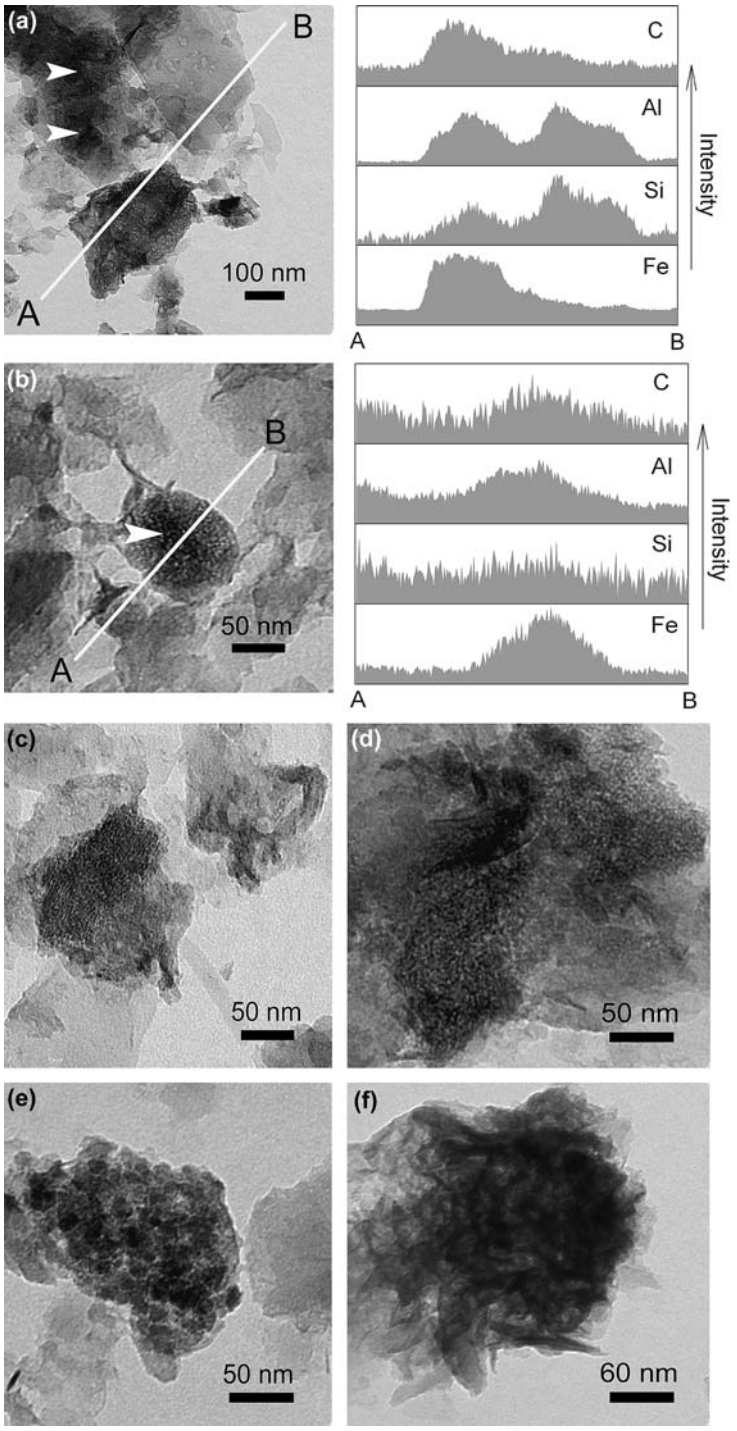
(a)
B
A
100 nm
C
Al
Si
Fe
Intensity
A
B
(b)
B
A
50 nm
C
Al
Si
Fe
Intensity
A
B
(c)
50 nm
(d)
50 nm
(e)
50 nm
(f)
60 nm

Figure 3. (a–f). TEM images and cross section element analysis of fine-clay fractions (<0.2 μm) of (a) the Chromic Cambisol Bw horizon (Sample 7) and (b) the Umbric Andosol Bw horizon (Sample 11) after NaOCl treatment. In sample 7, which has the highest Fe_o content of all studied samples, the signal intensities of stable OC were closely correlated with Fe signals ($r^2 = 0.95$) and less close with Al and Si signals ($r^2 = 0.59$ and 0.25, respectively). In contrast, in sample 11, which has the highest Al_o content of all samples, Fe and Al signals contributed similarly to the signal intensity of stable OC ($r^2 = 0.69$ and 0.70, respectively), while, again, Si signals showed the poorest correlation with the signals of stable OC ($r^2 = 0.45$). For analysis, 10,000 scans were collected; the electron beam thickness was ~20 nm; (c) and (d) Fe (hydr)oxides covering the surfaces of layered silicates in sample 7; (e) agglomerations of spherical crystals of Fe (hydr)oxides in sample 11; (f) microaggregate enriched in stable OC, Fe, Al, and Si in sample 11.

(mean value $40 \pm 14\%$) of the stable OC, which equaled 35–73% (mean value $55 \pm 13\%$) of the stable OC soluble in HF (Tables 1 and 3). Pyrophosphate-extractable stable OC was closely related to HF-extractable stable OC ($r^2 = 0.94$; $p < 0.001$). We also found significant correlations between MOC and Fe_p ($r^2 = 0.79$; $p < 0.001$), Al_p ($r^2 = 0.54$; $p < 0.01$) and $(Fe + Al)_p$ ($r^2 = 0.80$; $p < 0.001$; Figure 1c). When combining the amounts of Fe_p and Al_p with Fe_{d-o}, 90% of the variability of MOC could be explained (Equation 6; partial correlation coefficients and p values for Fe_p, Al_p, and Fe_{d-o} are: $r = 0.87$, $p < 0.01$; $r = 0.61$, $p < 0.06$; and $r = 0.64$, $p < 0.05$, respectively).

$$\mathrm{MOC}\ (\mathrm{g\,kg^{-1}}) = 1.12\ \mathrm{Fe_p} + 0.50\ \mathrm{Al_p} + 0.05\ \mathrm{Fe_{d-o}} + 1.29 \quad (R^2 = 0.90;\ p < 0.001; n = 12) \tag{6}$$

Table 3. Sodium-pyrophosphate-extractable Fe, Al and C, and atomic ratios of Na-pyrophosphate-extractable C and Fe plus Al as determined after NaOCl treatment.

No.	Fe_p (g kg^{-1})	Al_p (g kg^{-1})	C_p (g kg^{-1})	$C_p/(Fe+Al)_p$
1	0.6	0.6	1.2	3.2
2	0.5	0.9	1.3	2.5
3	0.3	0.6	0.8	2.3
4	0.2	0.8	2.7	6.5
5	1.0	1.0	1.9	2.8
6	1.6	1.4	2.3	2.3
7	10.4	5.0	12.5	2.8
8	2.1	1.5	2.1	1.8
9	5.9	7.9	8.3	1.7
10	4.3	6.6	5.0	1.3
11	3.1	8.4	8.4	1.9
12	3.3	1.6	4.8	3.4

Average analytical errors, expressed as coefficients of variation, of Fe_p, Al_p, and C_p among all twelve samples analyzed were 11, 11, and 8%.

In our subsoil samples, Fe_p and Fe_o covary, as do Al_p and Al_o ($r^2 = 0.73$ and 0.94, respectively). This covariance might be caused by the ability of both pyrophosphate and oxalate to extract goethite, gibbsite, amorphous $Al(OH)_3$, and ferrihydrite (Schuppli et al. 1983; Parfitt and Childs 1988; Kaiser and Zech 1996). The contribution of Fe and Al from inorganic sources could thus explain the similar R^2 in regression Equations 4 and 6.

After NaOCl treatment, the atomic $C_p/(Fe + Al)_p$ ratios ranged from 1.3 to 6.5 (mean at 2.7 ± 1.3) (Table 3). An atomic $C_p/(Fe + Al)_p$ ratio varying between 6 and 10 suggests that nearly all negative charges of OM were balanced by monomeric Fe and Al ions (Buurman 1985; Oades 1989). Therefore, functional groups of pyrophosphate-extractable stable OM were likely coordinated with polymeric Fe and Al species (e.g., hydroxides or ferrihydrite extracted by pyrophosphate). In summary, the resistance of MOC to NaOCl treatment resulted mainly from association with polymeric Fe and Al species, ferrihydrite and partly with crystalline Fe oxides (goethite, hematite). In samples containing chlorite or Al-hydroxy-interlayered vermiculite, protection of MOC by association with the Al-hydroxy phases seems also possible (Table 1). In contrast to MOC, the concentration of mineral-protected nitrogen (MN) was independent from all properties of the mineral phase that we analyzed, i.e., clay content, SSA, FR, Fe_{d-o}, Fe_d, Fe_o, $(Fe + Al)_o$, Al_o, and CEC of silicates.

Chemically resistant organic matter

Total amounts of chemically resistant organic carbon (ROC) varied widely among samples, ranging from 0.4–6.5 g kg^{-1} soil and accounting for 4–60% of stable OC, whereas the concentrations of resistant nitrogen (RN) were negligibly small (Table 2). On average $27 \pm 15\%$ of stable OC (Figure 1a) and $13 \pm 7\%$ of stable N was resistant to NaOCl and subsequent HF treatment. The C/N ratios of chemically washed OM were significantly wider than those of mineral-protected OM (mean difference of 19; $p < 0.01$) (Table 2). We did not find a significant relationship of ROC or RN with any variable of the mineral phase that we measured (i.e., clay content, SSA, FR, Fe_{d-o}, Fe_d, Fe_o, $(Fe + Al)_o$, Al_o, and CEC of silicates).

Radiocarbon content of organic matter pools

Table 4 shows radiocarbon data of OM fractions. Hypochlorite treatment always removed a younger OM fraction. In nine out of 12 samples, mass-balance calculations revealed that NaOCl preferentially removed OM enriched in 'bomb-^{14}C' from atmospheric nuclear weapon testing, even in deep horizons such as sample 4 (Humic Ferralsol; Bw). The decrease of $\Delta^{14}C$ values associated with the removal of OM by NaOCl correlated negatively with the concentration of oxalate-extractable Fe plus Al ($r^2 = 0.61$; $p < 0.01$; Figure 4).

Table 4. Isotopic properties of OM fractions.

No.	Untreated				NaOCl-removable				NaOCl-resistant			
	$\Delta^{14}C$ (‰)	pmC (%)	age (years)	$\delta^{13}C$ (‰)	$\Delta^{14}C$ (‰)	pmC (%)	age (years)	$\delta^{13}C$ (‰)	$\Delta^{14}C$ (‰)	pmC (%)	age (years)	$\delta^{13}C$ (‰)
1	−1.1	101 ± 0.4	modern[a]	−26.0	164.4	117 ± 1.3	modern	−25.4	−207.9	80 ± 0.3	1820 ± 35	−26.8
2	27.3	103 ± 0.4	modern	−25.1	104.0	111 ± 0.9	modern	−24.4	−106.0	90 ± 0.4	850 ± 40	−26.4
3	−124.2	88 ± 0.3	1015 ± 30	−24.9	51.1	106 ± 2.1	modern	−24.7	−306.9	70 ± 0.3	2895 ± 40	−25.1
4	−463.2	54 ± 0.3	4945 ± 50	−25.0	113.9	112 ± 4.9	modern	−33.7	−549.4	45 ± 0.3	6350 ± 60	−23.7
5	23.9	103 ± 0.4	modern	−24.9	80.8	109 ± 1.1	modern	−24.8	−103.0	90 ± 0.4	820 ± 35	−25.2
6	77.2	108 ± 0.5	modern	−25.8	113.3	112 ± 1.1	modern	−26.1	−15.5	99 ± 0.5	75 ± 40	−25.0
7	−57.5	95 ± 0.5	425 ± 45	−25.3	−13.1	99 ± 1.3	54 ± 52	−24.9	−90.6	92 ± 0.4	710 ± 35	−25.6
8	−48.2	96 ± 0.4	345 ± 40	−26.2	52.5	106 ± 0.8	modern	−26.2	−168.2	84 ± 0.4	1430 ± 40	−26.2
9	−80.9	93 ± 0.4	625 ± 40	−26.3	30.1	104 ± 0.7	modern	−26.3	−162.5	84 ± 0.4	1375 ± 40	−26.3
10	−377.8	63 ± 0.3	3760 ± 45	−24.4	−227.7	78 ± 0.7	2025 ± 38	−24.7	−489.5	51 ± 0.3	5350 ± 60	−24.2
11	−224.6	78 ± 0.4	1990 ± 45	−26.0	−168.3	84 ± 0.8	1429 ± 42	−26.3	−278.1	73 ± 0.4	2565 ± 45	−25.7
12	−37.8	97 ± 0.4	260 ± 35	−26.9	18.6	103 ± 1.7	modern	−26.8	−112.3	89 ± 0.4	905 ± 40	−27.0

No.	NaOCl-resistant							
	Released by HF (MOC)				Not released by HF (ROC)			
	$\Delta^{14}C$ (‰)	pmC (%)	age (years)	$\delta^{13}C$ (‰)	$\Delta^{14}C$ (‰)	pmC (%)	age (years)	$\delta^{13}C$ (‰)
1	−191.8	81 ± 2.8	1660 ± 30	−26.4	−247.1	76 ± 0.4	2225 ± 40	−27.7
2	−67.0	94 ± 2.2	506 ± 35	−25.9	−165.9	84 ± 0.4	1405 ± 40	−27.2
3	−292.9	71 ± 3.8	2734 ± 32	N.A.	−326.9	68 ± 0.4	3125 ± 45	N.A.
4	N.A.	N.A.	N.A.	N.A.	N.A.	N.A.	N.A.	N.A.
5	−89.2	92 ± 4.2	700 ± 30	−24.2	−129.8	88 ± 0.5	1065 ± 45	−27.1
6	62.7	107 ± 2.7	modern	−21.3	−66.8	94 ± 0.4	505 ± 40	−27.4
7	−76.1	93 ± 4.7	584 ± 32	−25.1	−147.5	86 ± 0.4	1230 ± 35	−27.4
8	−141.1	86 ± 1.7	1171 ± 37	−25.5	−245.7	76 ± 0.4	2215 ± 40	−28.1
9	−152.8	85 ± 0.8	1281 ± 37	−25.2	−185.2	82 ± 0.4	1595 ± 40	−28.8
10	−508.5	50 ± 0.7	5654 ± 54	N.A.	−348.1	66 ± 0.3	3385 ± 45	N.A.
11	−273.2	73 ± 1.5	2512 ± 36	−25.0	−298.1	71 ± 0.4	2790 ± 60	−28.4
12	−110.1	90 ± 40	886 ± 36	−26.9	−166.7	84 ± 0.5	1415 ± 40	−29.1

Data for untreated and NaOCl-resistant OC obtained from Kleber et al. (2005).
[a] = ^{14}C derived from aboveground-nuclear weapon testing.
N.A. = not available because insufficient amount of sample for analysis.

This result corroborates that OM with shorter residence time was more effectively protected against oxidative degradation and/or desorption in samples containing large amounts of poorly crystalline Fe and Al phases and metal hydroxy-OM complexes.

Following treatment with NaOCl, the $\Delta^{14}C$ value of the residual OM was more negative, corresponding to an average difference in radiocarbon age of about 960 years compared with untreated OM (Table 4). However, the ^{14}C content of the smectitic Vitric Phaeozem AB horizon (Sample 6) was, modern before and after NaOCl treatment albeit reaction with NaOCl resulted in the largest loss of OC (72%) in all samples studied. This implies that most of the stabilized OM in that soil was recently deposited. We rule out the influence of fresh detritus in this sample since no such material was detected by scanning electron microscopy (not shown). In summary, NaOCl removed OM with shorter residence time relative to the non-extracted OM in all studied subsoil horizons.

The $\Delta^{14}C$ values of mineral-protected OM were between 62.7 and $-508.5‰$, corresponding to conventional radiocarbon ages of modern to 5654 years, and those of chemically resistant OM ranged from -66.8 to $-348.1‰$, or 505–3385 years B.P. When omitting samples 4 (no material left for analysis) and 10 (Andic Luvisol; 2Bw), having lower $\Delta^{14}C$ values in the MOC than in the ROC faction, ROC had a significantly lower ^{14}C content than MOC (mean difference in age and $\Delta^{14}C$: ≈550 years and 65‰; both significant at $p < 0.001$,

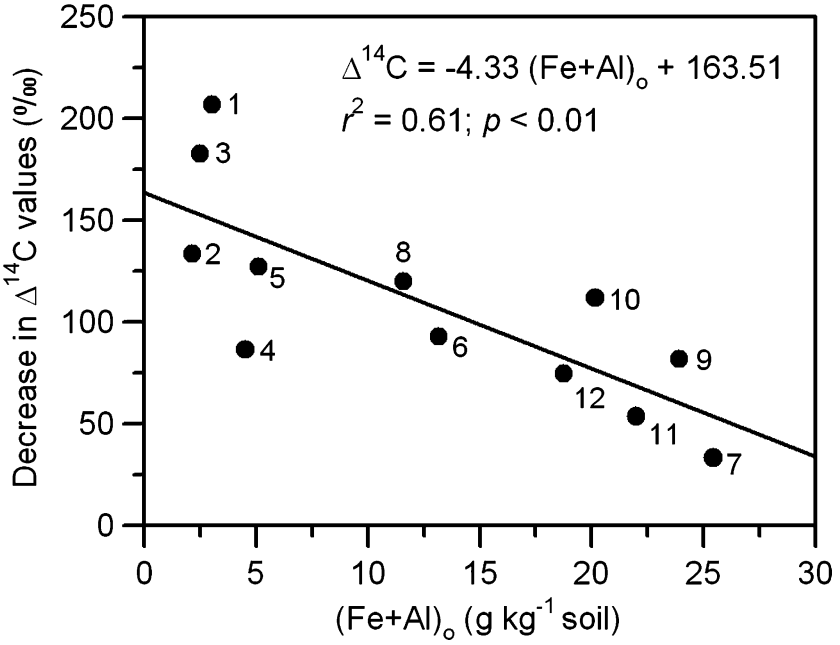

Figure 4. Decrease of $\Delta^{14}C$ values upon treatment of subsoil samples with NaOCl in relation to the content of oxalate-extractable Fe plus Al. Sample labeling corresponds to Table 1.

$n = 10$). This confirms that treatment of oxidized subsoils with 10% HF separated two OM fractions with different residence times. The $\Delta^{14}C$ values of MOC and ROC correlated negatively with mean horizon depth ($r^2 = 0.79$, $p < 0.001$; $r^2 = 0.59$, $p < 0.01$, $n = 11$). Mean ecosystem residence time increases with depth because of the transport time for plant inputs to reach lower horizons and due to slower decomposition with depth, where the latter is likely the result of environmental conditions that limit microbial activity (e.g., O_2 availability), as well as enhanced mineral-association that reduces the substrate availability to microbes (Paul et al. 1997; Kaiser et al. 2002). Multiple partial correlation analysis was used to separate the influence of horizon depth from other variables. In addition to being correlated with mean horizon depth (D), we observed a significant relationship of the $\Delta^{14}C$ values of MOC and ROC with SSA (Equations 7 and 8).

$$\Delta^{14}C_{MOC} = -5.45\ D + 4.08\ SSA - 87.09 \quad (7)$$

($R^2 = 0.88$; $p < 0.001$; $n = 11$; partial correlation coefficients and p values for mean horizon depth and SSA are: $r = -0.97$; $p < 0.001$ and $r = 0.65$; $p < 0.05$, respectively)

$$\Delta^{14}C_{ROC} = -2.97\ D + 3.74\ SSA - 204.81 \quad (8)$$

($R^2 = 0.81$; $p < 0.01$; $n = 11$; partial correlation coefficients and p values for mean horizon depth and SSA are: $r = -0.89$; $p < 0.001$ and $r = 0.73$; $p < 0.05$, respectively).

The positive relationship of SSA with $\Delta^{14}C$ values of MOC suggests that in samples with comparably large surface areas, most of which is provided by Fe (hydr)oxides (SSA vs. Fe_d: $r^2 = 0.64$; $p < 0.01$), also younger organic materials were stabilized by mineral surfaces. The relation of SSA with $\Delta^{14}C$ values of ROC (Equation 8) is presumably caused by the covariance between the $\Delta^{14}C$ values of MOC and ROC ($r^2 = 0.86$; $p < 0.001$). Except for SSA, no other mineral phase variable [clay content, FR, Fe_{d-o}, Fe_d, Fe_o, $(Fe + Al)_o$, Al_o] nor the ratios of Fe_d/Fe_t and Fe_{d-o}/Fe_t, which have been proposed to control ^{14}C ages of OM in Taiwanese soil profiles (Pai et al. 2004), had a significant linear relationship with the $\Delta^{14}C$ content of MOC or ROC.

^{13}C signatures

The $\delta^{13}C$ values of stable OM after NaOCl treatment did not differ consistently from untreated OM (Table 4). We observed more positive $\delta^{13}C$ values of MOC with increasing SSA ($r^2 = 0.46$; $p < 0.05$; $n = 9$), while the $\delta^{13}C$ values of ROC were independent of SSA. The ROC had significantly lower $\delta^{13}C$ values than MOC (mean difference = 2.8‰; $p < 0.001$, $n = 9$). The negative $\delta^{13}C$ values of ROC (−27.1 to −29.1‰) are consistent with relatively undecomposed plant inputs or the presence of aliphatic or lignin-derived substances (Benner et al. 1987; Lichtfouse et al. 1998; Krull and

Skjemstad 2003). However, the low $\Delta^{14}C$ values of ROC and the NMR results (see below) do not support the assumption that undecomposed plant remains caused the negative $\delta^{13}C$ values.

Contribution of lignin to stable organic matter

Table 5 gives the concentrations of lignin phenols in the OM fractions. Very little lignin was present in the untreated subsoil samples. The concentration of lignin-derived phenols (VSC) ranged from 4.3–33.5 g kg^{-1} OC and represented $<0.1\%$ of soil mass. The $\delta^{13}C$ values of untreated samples (-24.4 to $-26.9‰$; Table 4) and the mass ratios of syringyl–to–vanillyl units (S/V) of 0.11–0.65 (mean value 0.34 ± 0.17; not shown) suggest that the subsoil lignin mainly originated from tissues of gymnosperms (Sarkanen and Ludwig 1971; Onstad et al. 2000). Treatment with NaOCl dramatically reduced VSC contents (Table 5), which averaged 81% normalized to soil mass. In fact, lignin phenols were preferentially removed by NaOCl when compared with losses of bulk OC (Figure 5; Table 5). The lowest relative lignin loss was from the Bw horizon of the Ferralsol (Samples 4), which contains much clay and crystalline Fe oxides (Table 1). Additionally, the fraction of lignin phenols in stable OM (g VSC kg^{-1} OC) was on average 63% lower than in the initial samples. This confirms the preferential degradation of lignin, because non-preferential removal of lignin would not have altered the OC-normalized content of lignin phenols (Table 5).

Table 5. Contribution of lignin phenols (VSC) in OM fractions.

No.	Untreated		NaOCl-resistant					
			Total		Released by HF (MOC)		Not released by HF (ROC)	
	(g kg^{-1} soil)	(g kg^{-1} OC)	(g kg^{-1} soil)	(g kg^{-1} OC)	(g kg^{-1} soil)	(g kg^{-1} OC)	(g kg^{-1} soil)	(g kg^{-1} OC)
1	0.36	33.45	0.03	5.25	0.01	5.24	0.01	0.01
2	0.16	14.00	0.04	9.69	0.03	9.68	0.01	0.01
3	0.07	15.16	0.03	13.07	0.02	13.05	0.01	0.01
4	0.06	5.73	0.03	3.61	N.A.[a]	N.A.	N.A.	N.A.
5	0.24	12.17	0.01	1.51	0	1.49	0.01	0.01
6	0.63	16.39	0.02	2.03	0	0.75	0.02	1.28
7	0.51	14.25	0.07	3.37	0.05	3.33	0.02	0.03
8	0.22	15.75	0.03	4.14	0.02	4.04	0.01	0.10
9	0.34	11.01	0.04	1.99	0.01	1.96	0.03	0.03
10	0.07	4.29	0.03	3.26	0.02	3.22	0.01	0.04
11	0.22	8.19	0.03	2.23	0.01	2.08	0.02	0.15
12	0.31	13.21	0.03	2.67	0.03	2.67	0.002	0.002

[a]N.A. = not available because insufficient amount of sample for analysis.

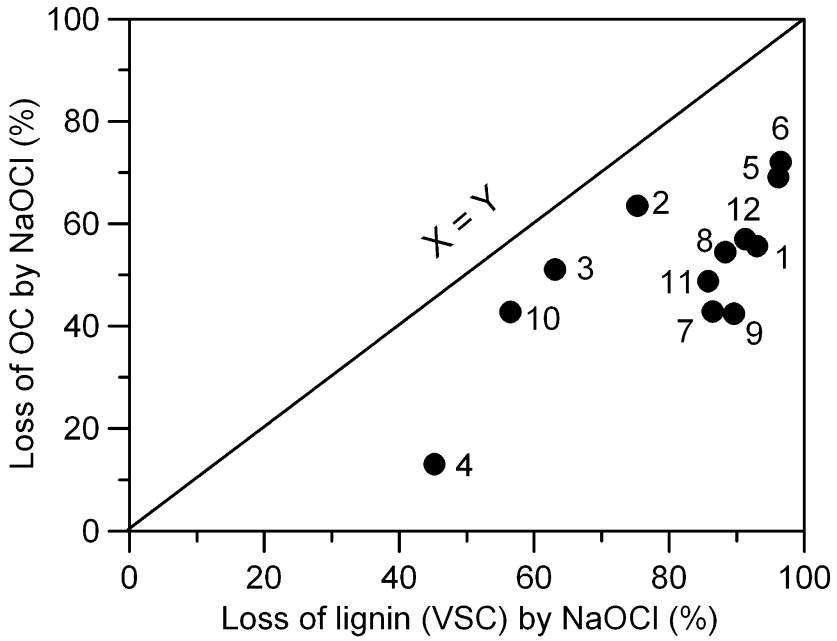

Figure 5. Relative losses of bulk OC and lignin phenols (VSC) during treatment with 6 wt% NaOCl. The percentage losses refer to the reduction of OC and VSC contents normalized to soil mass. Sample labeling corresponds to Table 1.

In consequence, much less than 13 g VSC per kg of stable OC was present after NaOCl treatment, implying no quantitatively important contribution of lignin to mineral-protected and recalcitrant OM in the subsoil samples. The HF treatment removed virtually all lignin-derived phenols (Table 5). On average, 4.3 ± 3.8 and 0.2 ± 0.4 g VSC per kg OC were present in the MOC and ROC fraction, respectively. These results and those from NMR suggest that the small stable lignin pool was likely protected by association with soil minerals rather than being chemically recalcitrant. However, no relationship between mineralogical properties [SSA, FR, Fe_{d-o}, Fe_d, Fe_o, $(Fe+Al)_o$, Al_o, CEC of silicates] and the (1) amount of NaOCl-resistant lignin (VSC), (2) HF-extractable VSC, and (3) non-HF-extractable VSC (per kg soil) was observed. Because of the insignificant amount of lignin in the ROC fraction, the relatively negative $\delta^{13}C$ values of ROC can tentatively be assigned to aliphatic materials rather than to lignin (Table 4).

Cross-polarization magic-angle spinning carbon-13 NMR

The ^{13}C-NMR spectra of OM after NaOCl plus HF treatment are shown in Figure 6 and the relative peak intensities are given in Table 6. Despite

differences in soil type, sampling depths, and mineral compositions, all the spectra appear similar. They exhibit strong resonances in the alkyl C (−10 to 45 ppm), O-alkyl C (60–90 ppm), and carboxyl C region (160–185 ppm), accounting for on average 56 ± 6%, 13 ± 2%, and 8 ± 1% of the total peak intensity, respectively (Table 6). The alkyl peaks show pronounced shoulders near 20 ppm, likely representing terminal CH_3–groups. Even when considering possible changes of the sp^2 and sp^3 carbon signal intensities by the CPMAS technique (Mao et al. 2000), the observed predominance of alkyl C is in agreement with the low $\delta^{13}C$ values, wide C/N ratios, and high atomic H/C

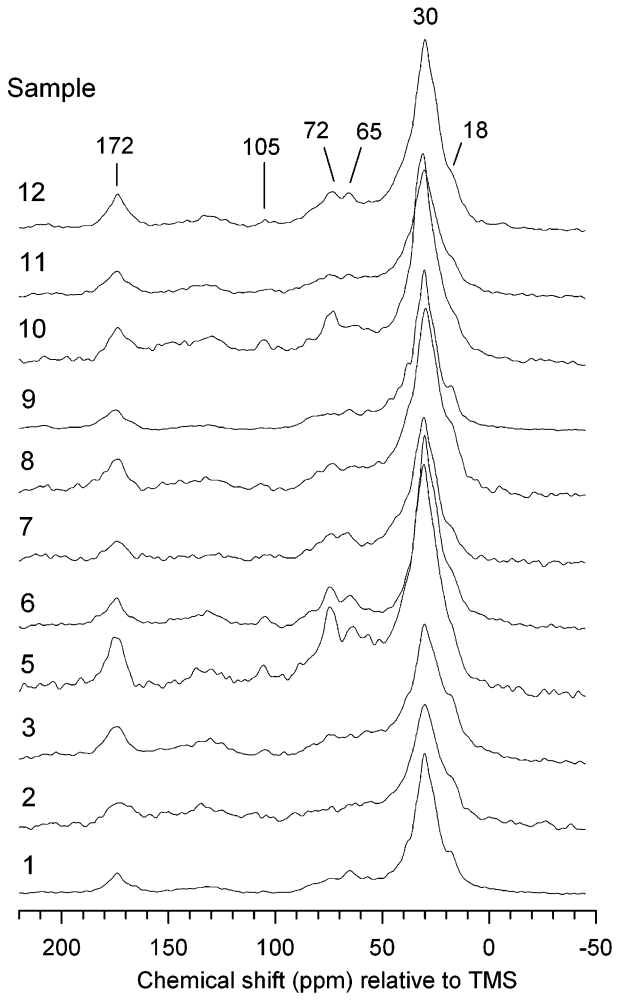

Figure 6. Solid-state CPMAS ^{13}C-NMR spectra of chemically resistant (recalcitrant) OM surviving sequential treatment with 6 wt% NaOCl and 10% HF. No spectrum was obtained of the Humic Ferralsol Bw horizon (Sample 4). Sample labeling corresponds to Table 1.

Table 6. Relative contribution of carbons to chemical shift regions of CPMAS ^{13}C-NMR spectra of chemically resistant (recalcitrant) OM (ROC) surviving treatment with NaOCl and HF (in%).

No.	Ketonic/Aldehyde C 185–220 ppm	Carboxyl C 160–185 ppm	Aryl C		Anomeric C 90–110 ppm	O-Alkyl C 60–90 ppm	Methoxyl/ N-Alkyl C 45–60 ppm	Alkyl C −10 to 45 ppm
			O-substituted 140–160 ppm	C-substituted 110–140 ppm				
1	1.9	7.2	1.9	4.3	1.0	11.5	6.9	65.1
2	2.0	8.6	5.1	10.3	4.2	11.1	7.6	51.1
3	4.2	9.2	4.3	8.4	2.9	11.0	8.0	52.1
4	Poorly resolved							
5	4.2	8.0	2.5	6.6	4.3	18.1	8.8	47.5
6	2.4	7.3	2.6	5.7	1.8	14.2	5.2	60.7
7	4.4	6.9	2.3	4.2	2.7	14.4	7.8	57.4
8	4.8	8.3	3.5	6.4	2.6	11.4	7.4	55.7
9	3.0	7.1	0.9	2.4	1.2	11.4	8.0	65.9
10	2.2	7.4	5.0	8.8	4.6	14.2	7.2	50.6
11	3.0	8.7	2.8	6.4	3.1	12.7	7.7	55.6
12	3.1	7.8	2.3	5.3	2.8	14.0	7.6	57.1

ratios of the ROC fraction although in some samples covalent-bonded H from inorganic sources contribute to unreasonably high H/C ratios (i.e., >2.5; Table 2).

Signals in the 45–60 ppm region contribute 7 ± 1% to the total peak intensity and can be assigned to methoxyl groups (R–O–CH_3) in lignin molecules, α-C of amino acids, or to tertiary/quaternary C atoms in branched aliphatic structures. We observed a positive relationship of the absolute amounts of methoxyl/N-alkyl C as derived from NMR with CuO-accessible lignin phenols (VSC per kg soil) ($r^2 = 0.91$, $p < 0.001$).

A significant fraction of HF-resistant C resonated in the 60–90 ppm region, indicating alcoholic (RC–OH) and ether bonds (RC–O–R) as present in polysaccharides or lignin side chains. This finding was most pronounced in the kaolinitic Chromic Cambisol Bw horizon (Sample 5; Table 6). The aryl C region (110–160 ppm) was characterized by broad peaks indicating only small contributions of aromatic compounds to chemically resistant OM (Figure 6). The contribution of O-substituted aryl C (160–140 ppm) was smaller (on average 3 ± 1% of total peak intensity) than that of C-substituted aromatic or unsaturated aliphatic compounds (140–110 ppm; average 6 ± 2% of total peak intensity). Resonances due to aryl C were almost absent in the spectrum of the Andic Luvisol Bt horizon (Sample 9), while they were most intense (15% of total signal intensity) in the spectrum of the Haplic Luvisol E horizon (Sample 2 in Figure 6). The presence of lignin phenols was again confirmed by positive correlations between the absolute amounts of O-aryl C and C-aryl C, with the amounts of lignin phenols (VSC per kg soil) ($r^2 = 0.53$, $p < 0.05$; $r^2 = 0.62$, $p < 0.01$, respectively). We exclude a significant contribution of signals derived from chlorinated compounds in the aliphatic and aromatic region (Hanna et al. 1991; Rajan et al. 1996). Chlorination by NaOCl decreases with pH, being maximal close to pH 2, whereas we conducted the NaOCl treatment at pH 8 (Lebedev et al. 2004). Given the poorly resolved signals derived from aromatic C, the high atomic H/C ratios and the fact that particulate black carbon was never observed by visual inspection, we infer that combusted materials were not important components of the chemically resistant OM in the studied subsoil horizons.

Discussion

Mineral-protected organic matter

Based on changes in ^{14}C and OC concentrations, we conclude that the NaOCl treatment was effective in removing soil OC with a relatively short residence time and left behind more stable OC (Kleber et al. 2005). Treating soils with HF can release large amounts of OC (up to 92%) from soils containing large contents of mineral-bound OM (Dai and Johnson 1999; Kaiser et al. 2002; Eusterhues et al. 2003; Gonçalvez et al. 2003). In our experiment, HF released

up to 96% of stable OC. On average, the 12 samples contained 73% mineral-protected OC and 27% recalcitrant OC (HF-resistant). Consequently, organo-mineral interactions played the major role in stabilizing OC in the studied soil horizons. If recalcitrant organic moieties associated with mineral-attached OM were not extracted by HF, the amount of mineral-protected OM would even be larger than reported in this study.

Nitrogen that survived the NaOCl treatment was effectively removed during mineral dissolution (average 87%), which is in accordance with results of Schmidt and Gleixner (2005), who also noted a preferential loss of N compared with C during HF treatment. Assuming that mineral-fixed NH_4^+ contributes little to stable N, the result indicates that N is mainly preserved in organo-mineral associations and not in recalcitrant OM. This is supported by small C/N ratios of MOC in four samples, suggesting a significant abundance of proteinaceous compounds (Table 2). In the present study, however, we obtained no indication that the HF-soluble stable N was preferentially associated with either Fe and Al (hydr)oxides or with the surfaces of silicates.

The significant positive relationship between SSA and $\delta^{13}C$ values of MOC reveals a trend that the HF treatment extracted ^{13}C-enriched OM preferably from those samples having large SSA due to the abundance of Fe and Al (hydr)oxides. By contrast, in samples with smaller SSA, which presumably contain less protective mineral phases, HF treatment released predominantly ^{13}C-depleted organic constituents. This finding agrees with the view that potentially biodegradable compounds enriched in ^{13}C such as polysaccharides and proteins can be stabilized by mineral surfaces (Bird et al. 2003; Kiem and Kögel-Knabner 2003) and are thus effectively removed during mineral dissolution (Dai and Johnson 1999; Schmidt and Gleixner 2005).

Plant lignin has been considered comparably resistant against microbial decomposition since only a limited group of fungi (white rot fungi) is capable of completely decomposing lignin to CO_2 (Kögel-Knabner 2002). Based on our observations that (1) lignin was preferentially removed by NaOCl and (2) NaOCl-removable OM had $\Delta^{14}C$ values indicating a modern radiocarbon age, we conclude that, in a quantitative sense, most of the subsoil lignin is not stabilized by association with minerals (even in horizons rich in poorly crystalline minerals), or by its complex phenylpropanoid structure. The slight contribution of lignin phenols to mineral-protected OM contrasts with the observation that poorly crystalline minerals such as ferrihydrite and Al hydroxide protected beach leaf litter lignin from mineralization during a 498-day incubation experiment (Miltner and Zech 1998). However, the limited protection of subsoil lignin is consistent with recent results obtained from surface soils showing that lignin is not a long-lived component of OM (Kiem and Kögel-Knabner 2003; Dignac et al. 2004).

According to Kaiser and Guggenberger (unpublished data), NaOcl is barely effective in removing OM directly attached to the surface of goethite. Given the strong relationships between MOC and mineral phase properties, and the TEM

results, we infer that OM in the subsoil samples, surviving exposure to NaOCl and being released by HF, was most significantly associated with polymeric Fe and Al species and with poorly crystalline Fe phases like ferrihydrite. Preferential association of OM with nuclei of polymeric Fe and Al (hydroxides) and poorly crystalline minerals (ferrihydrite, allophane, microcrystalline gibbsite) during the early stages of pedogenesis has been described previously for Hawaiian soils derived from volcanic ash materials (Chorover et al. 2004).

Our findings suggest that in the subsurface horizons of many different acid soils, there are amorphous or poorly crystalline phases present and involved in C stabilization, rather than being restricted to soils containing poorly crystalline aluminosilicates (allophane or imogolite-type minerals in Andosols or Podzols). This view is supported by Wiseman and Püttmann (2005), who showed that oxalate-extractable Fe and Al, especially Fe_o, were the best predictors of C stocks in temperate German soils. This finding also held true for a slightly alkaline Anthrosol/Vertisol/Gleysol-Chernozem profile (pH 7.3–7.8). In the samples we studied, Fe (hydr)oxides appeared to be more effective in C protection than were the Al-hydroxy phases.

In acid subsoil horizons, poorly crystalline minerals may originate from the weathering of primary minerals or from the degradation of (illuviated) metal-organic complexes and the subsequent hydrolysis and precipitation of released metals (Lundström et al. 2000; Masiello et al. 2004). The formation of amorphous and poorly crystalline mineral phases yields strong sorbents with large SSA and surface charge (Karltun et al. 2000). Given a density of 3.93 g cm^{-3}, the SSA of the 2–10-nm crystallites of Fe oxides found in samples 7 and 11 (Chromic Cambisol and Umbric Andosol) can be calculated to range from 150 to 760 m^2 g^{-1}. These values are similar to the results obtained by Eusterhues et al. (2005), who used selective extractions to estimate the average diameter of Fe oxides in two acidic soil profiles (Dystric Cambisol and Haplic Podzol) to be in the range of 2–7.5 nm and SSA values of up to 800 m^2 g^{-1} for ferrihydrite. Preferential sorption and clogging of micro- and small mesopores (2–10 nm) by OM has been reported for ferrihydrite and amorphous Al hydroxide (Kaiser and Guggenberger 2003; Mikutta et al. 2004). Organic matter bound with multiple ligands to micro- and mesoporous sorbents may be less susceptible to desorption and oxidative degradation (Zimmerman et al. 2004; Kaiser and Guggenberger 2003), and possibly also to biodegradation, because it is less available for microbes and enzymes.

Since polymeric Fe and Al species as well as poorly crystalline minerals appear abundant in the subsoil samples investigated, both mechanisms – sorption of OM to poorly crystalline minerals and complexation of OM with polymeric metal species – may be operating simultaneously. The age of MOC comprised a continuum from modern to 5654 years B.P. The relatively small difference in ^{14}C age between MOC and untreated OC in samples 6 and 7 (Vitric Phaeozem and Chromic Cambisol; Table 4) indicates that even recently deposited organic substances can be stabilized by interaction with mineral surfaces and thus be integral components of the mineral-protected carbon pool.

The low $\delta^{13}C$ and $\Delta^{14}C$ values and the aliphatic composition of ROC (48–66% alkyl C) lend support to our basic hypothesis that sequential treatment of soils with NaOCl and HF isolates a biologically less active, recalcitrant OM fraction. In the subsoil samples investigated, ROC contributed 2–20% to total (untreated) OC (mean at 12 ± 5%). Despite using samples spanning a wide range of mineralogical composition, including all major phyllosilicate species and varying contents of sesquioxides, the chemical composition of ROC in all samples was similar as revealed by ^{13}C-NMR. The preservation of alkyl C moieties during NaOCl and HF treatment agrees with findings that aliphatic structures are relatively resistant to chemical treatments like oxidation or acid hydrolysis (Hanna et al. 1991; Westerhoff et al. 1999, 2004; Chefetz et al. 2002). However, the fact that ROC also contained 11–18% polysaccharide-type C (O-alkyl C) following NaOCl treatment and HF extraction suggests that these polysaccharide-type materials were part of recalcitrant organic moieties. These could originate from glycolipid-like structures present in microbial cell wall biopolymers or cutinized hemicellulosic membranes (Almendros et al. 1998). It is unlikely that resistant ligno-cellulose or lignin-polysaccharide structures contributed to the signals in the 60–90 ppm region since the ROC fraction contained almost no lignin phenols.

Although Jandl et al. (2004) obtained indications that aliphatic compounds in a Haplic Chernozem Ap horizon were associated with mineral surfaces, as shown by a significant correlation of SSA with the concentration of *n*-alkyl fatty acids, the size of the ROC pool in our samples was independent from SSA and sesquioxide contents. Therefore, in the samples investigated, most aliphatic compounds were probably present either free or encapsulated in organic structures (Lichtfouse 1998; Guignard et al. 2005). However, we cannot rule out that some aliphatic compounds were present as recalcitrant domains in organic materials associated with minerals.

Possible sources of alkyl C are aliphatic biopolymers from microbial cells, above-ground plant tissues like cutin and cutan (Nip et al. 1986), or suberin from plant roots (Tegelaar et al. 1995; Nierop 1998). For five acid subsoil B horizons under forest (*Fagus sylvatica*; *Picea abies*), Riederer et al. (1993) showed that cutin- or suberin-derived aliphatics can contribute between 0.4–2 g kg^{-1} soil, which is similar to the concentration of ROC observed in this study. The alkyl C in the ROC fraction may also originate from more humified substances like humic acids, which also contain $(CH_2)_n$ chains (e.g., Hu et al. 2000).

In the subsoil samples, the ^{14}C age of ROC was older than that of untreated OM and older (in all but one sample) than that of MOC. The long residence time and the predominance of alkyl C in our samples supports the view that aliphatic compounds are selectively preserved during biodegradation and thus are one of the oldest components of OM. Bol et al. (1996) and Huang et al. (1999) also found that aliphatic hydrocarbons were the oldest component of

OM in soils, being similar in age or older than the residuum surviving acid hydrolysis. Similarly, in the Atlantic and Pacific Oceans, Loh et al. (2004) observed significantly higher ^{14}C ages of lipophilic dissolved OM as compared with proteinaceous and carbohydrate-like OM, denoting that lipid-type structures also control the biological recalcitrance of OM in environments without protective mineral phases.

Conclusion

Sequential treatment of subsoils with NaOCl and HF has the potential to provide estimates of the pool size of mineral-protected and recalcitrant OM, and of the chemical composition of recalcitrant materials. Most of the stable OC (on average 73%) was associated with the soil mineral phase rather than being recalcitrant, but the recalcitrant fraction had on average longer mean residence times. The modern $\Delta^{14}C$ value of mineral-protected OM in the Vitric Phaeozem AB horizon shows that even recently deposited plant inputs may be stabilized by interaction with minerals. Reliance on hydrolysis for quantifying stable OM overlooks an important stabilization mechanism, because the non-hydrolysable fraction does not represent mineral-protected OC, and yet OC stabilized by minerals appears to be the dominant form of stable OC below the A horizon in many soils. The dominant mechanism of OM stabilization was association with polymeric Fe and Al hydroxides, ferrihydrite, and, in part, with crystalline Fe oxides. It appears that aliphatic structures make up a large fraction of non-mineral stabilized OC, whereas lignin is labile and not contained significantly in either mineral-associated or recalcitrant OM.

Acknowledgements

We are grateful to Klaus Kaiser for advice and discussion, Heike Knicker (Technical University Munich, Freising, Germany) for conducting the ^{13}C-NMR analysis, and Jörn Kasbohm and Manfred Zander for the TEM analysis (Ernst-Moritz-Arndt University, Greifswald, Germany). This study was funded by the Deutsche Forschungsgemeinschaft priority program SPP 1090 'Soils as sources and sinks for atmospheric CO_2', and partially supported by U.S. Department of Energy, Office of Science, under Contract No. DOE-AC03-76SF00098.

References

Almendros G., Guadalix M.E., Gonzalez-Vila F.J. and Martin F. 1998. Distribution of structural units in humic substances as revealed by multi-step selective degradations and C-13-NMR of successive residues. Soil Biol. Biochem. 30: 755–765.

Amelung W., Flach K.W. and Zech W. 1999. Lignin in particle-size fractions of native grassland soils as influenced by climate. Soil Sci. Soc. Am. J. 63: 1222–1228.

Baldock J.A. and Skjemstad J.O. 2000. Role of the soil matrix and minerals in protecting natural organic materials against biological attack. Org. Geochem. 31: 697–710.

Balesdent J. 1996. The significance of organic separates to carbon dynamics and its modeling in some cultivated soils. Eur. J. Soil Sci. 47: 485–493.

Benner R., Fogel M.L., Sprague E.K. and Hodson R.E. 1987. Depletion of ^{13}C in lignin and its implication for stable isotope studies. Nature 320: 708–710.

Bird M., Kracht O., Derrien D. and Zhou Y. 2003. The effect of soil texture and roots on the stable carbon isotope composition of soil organic carbon. Aust. J. Soil Sci. 41: 77–94.

Blakemore L.C., Searle P.L. and Daly B.K. 1987. Methods for Chemical Analysis of Soils. New Zealand Soil Bureau Scientific Report 80. NZ Soil Bureau, Department of Scientific and Industrial Research, Lower Hutt, New Zealand.

Bol R., Huang Y., Meridith J.A., Eglinton G., Harkness D.D. and Ineson P. 1996. The ^{14}C age and residence time of organic matter and its lipid constituents in a stagnohumic gley soil. Eur. J. Soil Sci. 47: 215–222.

Bracewell J.M., Campbell A.S. and Mitchell B.D. 1970. An assessment of some thermal and chemical techniques used in the study of the poorly-ordered aluminosilicates in soil clays. Clay Min. 8: 325–335.

Brunauer S., Emmett P.H. and Teller E. 1938. Adsorption of gases in multimolecular layers. J. Am. Chem. Soc. 60: 309–319.

Buurman P. 1985. Carbon/sesquioxide ratios in organic complexes and the transition albic-spodic horizon. J. Soil Sci. 36: 255–260.

Chefetz B., Salloum M.J., Deshmukh A.P. and Hatcher P.G. 2002. Structural components of humic acids as determined by chemical modifications and carbon-13 NMR, pyrolysis-, and thermochemolysis-gas chromatography/mass spectrometry. Soil Sci. Soc. Am. J. 66: 1159–1171.

Chorover J., Amistadi M.K. and Chadwick O.A. 2004. Surface charge evolution of mineral-organic complexes during pedogenesis in Hawaiian basalt. Geochim. Cosmochim. Acta. 68: 4859–4876.

Cuypers C., Grotenhuis T., Nierop K.G.J., Franco E.M., de Jager A. and Rulkens W. 2002. Amorphous and condensed organic matter domains: the effect of persulfate oxidation on the composition of soil/sediment organic matter. Chemosphere 48: 919–931.

Dai K.H. and Johnson C.E. 1999. Applicability of solid-state C CP/MAS NMR analysis in Spodosols: chemical removal of magnetic materials. Geoderma 93: 289–310.

Dignac M.-F., Bahri H., Rumpel C., Basse D.P., Bardoux G., Balesdent J., Girardin C., Chenu C. and Mariotti A. 2004. Carbon 13-C abundance as a tool to study the dynamics of lignin monomers in soil: an appraisal at the Closeaux experimental field (France). Geoderma 128: 3–17.

Eusterhues K., Rumpel C. and Kögel-Knabner I. 2005. Organo-mineral associations in sandy acid forest soils: importance of specific surface area, iron oxides and micropores. Eur. J. Soil Sci. (in press).

Eusterhues K., Rumpel C., Kleber M. and Kögel-Knabner I. 2003. Stabilization of soil organic matter by interactions with minerals as revealed by mineral dissolution and oxidative degradation. Org. Geochem. 34: 1591–1600.

FAO 1994. Soil Map of the World, revised legend, with corrections and updates. World Soil Resources Report 60, FAO, Rome, 1988. Reprinted with updates as: Technical paper 20, ISRIC, Wageningen, Netherlands.

Gonçalves C.N., Dalmolin R.S.D., Dick D.P., Knicker H., Klamt E. and Kögel-Knabner I. 2003. The effect of 10% HF treatment on the resolution of CPMAS ^{13}C NMR spectra and on the quality of organic matter in Ferralsols. Geoderma 116: 373–392.

Guggenberger G. and Kaiser K. 2003. Dissolved organic matter in soils. Challenging the paradigm of sorptive preservation. Geoderma 113: 293–310.

Guignard C., Lemée L. and Amblès A. 2005. Lipid constituents of peat humic acids and humin. Distinction from directly extractable bitumen components using TMAH and TEAAc thermochemolysis. Org. Geochem. 36: 287–297.

Hanna J.W., Johnson W.D., Querada R.A., Wilson M.A. and Xlao-Qlaot L. 1991. Characterization of aqueous humic substances before and after chlorination. Environ. Sci. Techn. 25: 1060–1064.

Hu W.G., Mao J.D., Xing B.S. and Schmidt-Rohr K. 2000. Poly(methylene) crystallites in humic substances detected by nuclear magnetic resonance. Environ. Sci. Techn. 34: 530–534.

Huang Y., Li B.C., Bryant C., Bol R. and Eglinton G. 1999. Radiocarbon dating of aliphatic hydrocarbons: a new approach for dating passive-fraction carbon in soil horizons. Soil Sci. Soc. Am. J. 63: 1181–1187.

Jandl G., Leinweber P., Schulten H.-R. and Eusterhues K. 2004. The concentrations of fatty acids in organo-mineral particle-size fractions of a Chernozem. Eur. J. Soil Sci. 55: 459–470.

Jastrow J.D., Boutton T.W. and Miller R.M. 1996. Carbon dynamics of aggregate-associated organic matter estimated by carbon-13 natural abundance. Soil Sci. Soc. Am. J. 60: 801–807.

Jones D.L. and Edwards A.C. 1998. Influence of sorption on the biological utilization of two simple carbon substrates. Soil Biol. Biochem. 30: 1895–1902.

Kaiser K. and Guggenberger G. 2003. Mineral surfaces and soil organic matter. Eur. J. Soil Sci. 54: 1–18.

Kaiser K. and Zech W. 1996. Defects in estimation of aluminum in humus complexes of podzolic soils by pyrophosphate extraction. Soil Sci. 161: 452–458.

Kaiser K., Eusterhues K., Rumpel C., Guggenberger G. and Kögel-Knabner I. 2002. Stabilization of organic matter by soil minerals – investigations of density and particle-size fractions from two acid forest soils. J. Plant Nutr. Soil Sci. 165: 451–459.

Kalbitz K., Schwesig D., Rethemeyer J. and Matzner E. 2005. Stabilization of dissolved organic matter by sorption to the mineral soil. Soil Biol. Biochem. 37: 1319–1331.

Karltun E., Bain D.C., Gustafsson J.P., Mannerkoski H., Murad E., Wagner U., Fraser A.R., McHardy W.J. and Starr M. 2000. Surface reactivity of poorly-ordered minerals in podzol B horizons. Geoderma 94: 265–288.

Karltun E. 1998. Modelling SO_4^{2-} surface complexation on variable charge minerals: II. Competition between SO_4^{2-}, oxalate and fulvate. Eur. J. Soil Sci. 49: 113–120.

Kiem R. and Kögel-Knabner I. 2003. Contribution of lignin and polysaccharides to the refractory carbon pool in C-depleted arable soils. Soil Biol. Biochem. 35: 101–118.

Kleber M., Mikutta R., Torn M.S. and Jahn R. 2005. Poorly crystalline mineral phases protect organic matter in acid subsoil horizons. Eur. J. Soil Sci. (in press) doi:10.1111/j.1365-2389.2005.00706.x.

Knicker H. and Lüdemann H.-D. 1995. N-15 and C-13 CPMAS and solution NMR studies of N-15 enriched plant material during 600 days of microbial degradation. Org. Geochem. 23: 329–341.

Kögel-Knabner I. 2002. The macromolecular organic composition of plant and microbial residues as inputs of soil organic matter. Soil Biol. Biochem. 34: 139–162.

Krull E.S. and Skjemstad J.O. 2003. $\delta^{13}C$ and $\delta^{15}N$ profiles in ^{14}C-dated oxisol and vertisols as a function of soil chemistry and mineralogy. Geoderma 112: 1–29.

Krull E.S., Baldock J.A. and Skjemstad J.O. 2003. Importance of mechanisms and processes of the stabilization of soil organic matter for modeling carbon turnover. Funct. Plant Biol. 30: 207–222.

Leavitt S.W., Follett R.F. and Paul E.A. 1996. Estimation of slow and fast-cycling soil organic carbon pools from 6 N HC1 hydrolysis. Radiocarbon 38: 231–239.

Lebedev A.T., Shaydullina G.M., Sinikova N.A. and Harchevnikova N.V. 2004. GC–MS comparison of the behavior of chlorine and sodium hypochlorite towards organic compounds dissolved in water. Water Res. 38: 3713–3718.

Leinweber P. and Schulten H.-R. 2000. Nonhydrolyzable forms of soil organic nitrogen: extractability and composition. J. Plant Nutr. Soil Sci. 163: 433–439.

Lichtfouse E. 1998. Plant wax n-alkanes trapped in soil humin by non-covalent bonds. Naturwiss. 85: 449–452.

Lichtfouse E., Chenu C., Baudin F., Leblond C., Da Silva M., Behar F., Derenne S., Largeau C., Wehrung P. and Albrecht P. 1998. A novel pathway of soil organic matter preservation by

selective preservation of resistant straight-chain biopolymers: chemical and isotope evidence. Org. Geochem. 28: 411–415.

Lilienfein J., Qualls R.G., Uselman S.M. and Bridgham S.D. 2004. Adsorption of dissolved organic carbon and nitrogen in soils of a weathering chronosequence. Soil Sci. Soc. Am. J. 68: 392–405.

Loh A.N., Bauer J.E. and Druffel E.R.M. 2004. Variable ageing and storage of dissolved organic components in the open ocean. Nature 430: 877–881.

Lundsröm U.S., van Breemen N., Bain D.C., van Hees P.A.W., Giesler R., Gustaffson J.P., Ilvesniemi H., Karltun E., Melkerud P.-A., Olsson M., Riise G., Wahlberg O., Bergelin A., Bishop K., Finlay R., Jongmans A.G., Magnusson T., Mannerkoski H., Nordgren A., Nyberg L., Starr M. and Tau Strand L. 2000. Advances in understanding the podzolization process resulting from a multidisciplinary study of three coniferous forest soils in the Nordic Countries. Geoderma 94: 335–353.

Mao J.D., Hu W.G., Schmidt-Rohr K., Davies G., Ghabbour E.A. and Xing B. 2000. Quantitative characterization of humic substances by solid-state carbon-13 nuclear magnetic resonance. Soil Sci. Soc. Am. J. 64: 873–884.

Masiello C.A., Chadwick O.A., Southon J., Torn M.S. and Harden J.W. 2004. Weathering controls on mechanisms of carbon storage in grassland soils. Global Biogeochem. Cycles 18 GB4023 10.1029/2004GB002219.

Mikutta R., Kleber M., Kaiser K. and Jahn R. 2005. Review: organic matter removal from soils using hydrogen peroxide, sodium hypochlorite and disodium peroxodisulfate. Soil Sci. Soc. Am. J. 69: 120–136.

Mikutta C., Lang F. and Kaupenjohann M. 2004. Soil organic matter clogs mineral pores: evidence from ^{1}H-NMR and N_2 adsorption. Soil Sci. Soc. Am. J. 68: 1853–1862.

Miltner A. and Zech W. 1998. Beech leaf litter lignin degradation and transformation as infuenced by mineral phases. Org. Geochem. 28: 457–463.

Nierop K.G.J. 1998. Origin of aliphatic compounds in a forest soil. Org. Geochem. 29: 1009–1016.

Nip M., Tegelaar E.W., Brinkhuis H., De Leeuw J.W., Schenk P.A. and Holloway P.J. 1986. Analysis of modern and fossil plant cuticules by Curie point Py-GC and Curie point Py-GC-MS: recognition of a new, highly aliphatic and resistant biopolymer. Org. Geochem. 10: 769–778.

Oades J.M. 1989. An introduction to organic matter in mineral soils. In: Dixon J.B. and Weed S.B. (eds), Minerals in Soil Environments, 2nd ed. SSSA Book Series Nr. 1, Madison, WI, pp. 89–160.

Omueti J.A.I. 1980. Sodium hypochlorite treatment for organic matter destruction in tropical soils of Nigeria. Soil Sci. Soc. Am. J. 44: 878–880.

Onstad G.D., Canfield D.E., Quay P.D. and Hedges J.I. 2000. Sources of particulate organic matter in rivers from the continental USA: lignin phenol and stable isotope composition. Geochim. Cosmochim. Acta 64: 3539–3546.

Pai C.-W., Wang M.-K., Zhuang S.-Y. and King H.-B. 2004. Free and non-crystalline Fe-oxides to total iron concentration ratios correlated with ^{14}C ages of three forest soils in Central Taiwan. Soil Sci. 169: 582–589.

Parfitt R.L. and Childs C.W. 1988. Estimation of forms of Fe and Al: a review, and analysis of contrasting soils by dissolution and Mössbauer methods. Aust. J. Soil Res. 26: 121–144.

Paul E.A., Collins H.P. and Leavitt S.W. 2001. Dynamics of resistant soil carbon of midwestern agricultural soils measured by naturally occurring C-14 abundance. Geoderma 104: 239–256.

Paul E.A., Follett R.F., Leavitt S.W., Halvorson A., Peterson G.A. and Lyon D.J. 1997. Radiocarbon dating for determination of soil organic matter pool sizes and dynamics. Soil Sci. Soc. Am. J. 61: 1058–1067.

Poirier N., Derenne S., Balesdent J., Mariotti A., Massiot D. and Largeau C. 2003. Isolation and analysis of the non-hydrolysable fraction of a forest soil and an arable soil (Lacadée, southwest France). Eur. J. Soil Sci. 54: 243–255.

Rajan P.S., Chen C.-L. and Gratzl J.S. 1996. Formation of chloro-organics during chlorine bleaching of softwood Kraft pulp. Holzforschung 50: 165–174.

Riederer M., Matzke K., Ziegler F. and Kögel-Knabner I. 1993. Occurrence, distribution and fate of the lipid plant biopolymers cutin and suberin in temperate forest soils. Org. Geochem. 20: 1063–1076.

Rutherford D.W., Chiou C.T. and Eberl D.D. 1997. Effects of exchanged cation on the microporosity of montmorillonite. Clays Clay Min. 45: 534–543.

Sarkanen K.V. and Ludwig C.H. 1971. Lignins. John Wiley & Sons, New York.

Schmidt M.W.I. and Gleixner G. 2005. Carbon and nitrogen isotope composition of bulk soils, particle-size fractions and organic material after treatment with hydrofluoric acid. Eur. J. Soil Sci. 56: 407–416.

Schuppli P.A., Ross G.J. and McKeague J.A. 1983. The effective removal of suspended materials from pyrophosphate extracts of soils from tropical and temperate regions. Soil Sci. Soc. Am. J. 47: 1026–1032.

Six J., Bossuyt H., Degryze S. and Denef K. 2004. A history of research on the link between (micro)aggregates, soil biota, and soil organic matter dynamics. Soil Till. Res. 79: 7–31.

Six J., Conant R.T., Paul E.A. and Paustian K. 2002. Stabilization mechanisms of soil organic matter: implications for C-saturation of soils. Plant Soil 241: 155–176.

Sollins P., Homann P. and Caldwell B.A. 1996. Stabilization and destabilization of soil organic matter: mechanisms and controls. Geoderma 74: 65–105.

Springob G. and Kirchmann H. 2002. C-rich sandy Ap horizons of specific historical land-use contain large fractions of refractory organic matter. Soil Biol. Biochem. 34: 1571–1581.

Stuiver M. and Polach H.A. 1977. Reporting of ^{14}C data. Radiocarbon 19: 355–363.

Tan Z.X., Lal R., Izaurralde R.C. and Post W.M. 2004. Biochemically protected soil organic carbon at the North Appalachian experimental watershed. Soil Sci. 196: 423–433.

Tegelaar E.W., Hollman G., Van der Vegt P., De Leeuw J.W. and Holloway P.J. 1995. Chemical characterization of the periderm tissue of some angiosperm species – recognition of an insoluble, nonhydrolyzable, aliphatic biomacromolecule (suberan). Org. Geochem. 23: 239–251.

Theng B.K.G., Tate K.R. and Becker-Heidmann P. 1992. Towards establishing the age, location, and identity of the inert soil organic matter of a spodosol. Z. Pflanzenernähr. Bodenkd. 155: 181–184.

Torn M.S., Trumbore S.E., Chadwick O.A., Vitousek P.M. and Hendricks D.M. 1997. Mineral control of soil organic carbon storage and turnover. Nature 389: 170–173.

Van Hees P.A.W., Vinogradoff S.I., Edwards A.C., Godbold D.L. and Jones D.L. 2003. Low molecular weight organic acid adsorption in forest soils: effects on soil solution concentrations and biodegradation rates. Soil Biol. Biochem. 35: 1015–1026.

Westerhoff P., Chao P. and Mash H. 2004. Reactivity of natural organic matter with aqueous chlorine and bromine. Water Res. 38: 1502–1513.

Westerhoff P., Aiken G., Amie G. and Debroux J. 1999. Relationships between the structure of natural organic matter and its reactivity towards molecular ozone and hydroxyl radicals. Water Res. 33: 2265–2276.

Wiseman C.L.S. and Püttmann W. 2005. Soil organic carbon and its sorptive preservation in central Germany. Eur. J. Soil Sci. 56: 65–76.

Zimmerman A.R., Chorover J., Goyne K.W. and Brantley S.L. 2004. Protection of mesopore-adsorbed organic matter from enzymatic degradation. Environ. Sci. Techn. 38: 4542–4548.